JOURNAL OF GEOPHYSICAL RESEARCH, VOL. 106, NO. C3, PAGES 4437–4448, MARCH 15, 2001

Autumn sea ice thickness, ridging and heat flux variability in and adjacent to Terra Nova Bay, Ross Sea, Antarctica

Martin O. Jeffries, Kim Morris, Ted Maksym, Nickolai Kozlenko, and Tina Tin

Geophysical Institute, University of Alaska Fairbanks, Fairbanks, Alaska

Abstract. The variability of sea ice thickness and snow depth observed from the R/V *Nathaniel B. Palmer* in late May 1998 in and adjacent to Terra Nova Bay (TNB), Ross Sea, Antarctica, is described. Conductive heat fluxes are estimated on the basis of the observed snow and ice thicknesses. There was only 6% areal coverage of open water in TNB and 87% of the areal coverage of unridged ice was ≤0.3 m thick. Between the western and eastern margins of TNB there were increases in the area-weighted unridged ice thickness (0.05-0.25 m) and the areal extent of ridging (2.5-18.5%). Ridged ice accounted for 44-66% of the total ice mass in TNB and was as vital to thickening the ice cover as it was outside the bay, where 30-60% of the total ice mass was contained within the 5-35% of ice that was ridged. Satellite passive microwave (Special Sensor Microwave Imager SSM/I) data show that the extensive ice cover in TNB was normal for this time of year probably because of the blocking effect of thick, ridged, 100% concentration pack ice outside the bay. Despite the extensive ice cover in TNB, there was an order of magnitude difference in area-weighted mean heat flux between the bay and the pack ice. For example, depending on the choice of bulk snow thermal conductivity value k_s (0.14 or 0.31 W m^{-1} K^{-1}), the heat flux values for unridged ice were 199 or 216 W m^{-2} in TNB versus 35 or 49 W m^{-2} on the inbound pack ice leg and 20 or 39 W m^{-2} on the outbound pack ice leg. Factoring in the contribution of ridges to the ice thickness distribution decreased the heat flux in the bay and the pack ice by 25 or 36%, depending on k_s. The greatest proportion of the heat flux in TNB occurred through the ice; no more than 30% of the heat loss was from open water. Since the ice conditions observed in TNB were apparently normal for the time of year, the heat fluxes also must have been quite normal.

1. Introduction

Polynyas are oceanic areas that remain either partially or totally free of ice at times and under meteorological conditions when the water surface would be expected to be totally covered with ice [*World Meteorological Organization (WMO)*, 1970]. Coastal polynyas are common around the margin of the Antarctic continent [*Kurtz and Bromwich,* 1985; *Cavalieri and Martin,* 1985; *Zwally et al.,* 1985; *Kottmeier and Engelbart,* 1992; *Adolphs and Wendler,* 1995; *Bromwich et al.,* 1998; *Markus et al.,* 1998; *Massom et al.,* 1998a; *Van Woert,* 1999a, 1999b]. They are often referred to as latent heat polynyas because the heat required to balance loss to the atmosphere, and hence to maintain the open water, is provided by the latent heat of fusion of continuous ice formation and removal. Because large quantities of sea ice are produced, polynyas are often referred to as "ice factories." Ice growth and ocean to atmosphere heat transfer are accompanied by salt injection into the ocean and subsequent dense water formation.

Terra Nova Bay (TNB) in the western Ross Sea, Antarctica, is the location of a prominent coastal polynya. According to *Bromwich and Kurtz* [1984] and *Kurtz and Bromwich* [1983, 1985] it is maintained solely by strong katabatic winds that blow sea ice offshore, while the blocking effect of the Drygalski Ice Tongue prevents sea ice drifting in from the south. *Van Woert* [1999a, 1999b] suggests that fluctuations in the extent of the polynya are also influenced by the compactness of the pack ice in the southwestern Ross Sea. The cumulative annual ice production in the TNB polynya has been estimated to be of the order of 50-80 km^3, amounting to an estimated 10% of the total ice production on the Ross Sea continental shelf [*Kurtz and Bromwich,* 1985; *Van Woert,* 1999a]. The resultant brine rejection contributes to High Salinity Shelf Water (HSSW) formation, which may amount to 20% of all shelf water in the Ross Sea [*Jacobs et al.,* 1985; *Kurtz and Bromwich,* 1985]. Export of HSSW from TNB polynya has been estimated to be 1 Sv [*Manzella et al.,* 1999; *Van Woert,* 1999b].

The investigation of TNB and other Antarctic coastal polynyas has relied primarily on remote sensing and numerical modeling, as few observations have been made in situ. Surface observations of polynya ice characteristics and processes are important as they can contribute to improvements in remote sensing of polynyas, forcing and validation of numerical models of their extent and ice production, and estimates of ocean-atmosphere exchanges. Observations from the R/V *Polarstern* in late 1986 revealed that the ice cover in Weddell Sea coastal polynyas thickened thermodynamically by both congelation and frazil ice growth and dynamically by rafting and ridging [*Eicken and Lange,* 1989]. The turbulent heat fluxes in those polynyas were subsequently calculated on the basis of the observed ice and meteorological conditions [*Kottmeier and Engelbart,* 1992]. An experiment aboard the R/V *Aurora Australis* in the Mertz Glacier polynya,

Paper number 1999JC000021.
0148-0227/01/1999JC000021$09.00

East Antarctica, in July and August 1999 will no doubt add significantly to the understanding of the nature of the ice cover and its influence on heat flow from polynyas.

In late May 1998 we made the first systematic ship-based observations of the autumn sea ice cover in and adjacent to TNB. This paper (1) describes snow and ice thickness variability in TNB and in the pack ice for a distance of 275 km east of the bay and (2) presents estimates of the conductive heat flux to the atmosphere as a function of the observed snow and ice thicknesses. There was very little open water in TNB: it was almost completely covered with moderately thick, ridged ice. These observations are placed in a longer temporal context (autumn 1988 through autumn 1998) using Special Sensor Microwave Imager (SSM/I) satellite passive microwave data to describe the open water/ice concentration variability and automatic weather station (AWS) data to describe air temperature and wind speed variability. The remote sensing and AWS data indicate that there was nothing unusual about the state of TNB and thus the heat flux estimates, for the time of year.

2. Study Area and Cruise Track

In May and June 1998 the R/V *Nathaniel B. Palmer* operated in the Ross Sea pack ice supporting sea ice geophysics and ecology investigations between the ice edge and the continent, primarily between 65° and 78°S and between 175°E and 175°W (Figure 1). The cruise included an excursion into and out of TNB, which is bordered on its south side by the Drygalski Ice Tongue, on its north side by Cape Washington, and on its west side by Nansen Ice Shelf, from which Hells Gate Ice Shelf is derived (Figure 1). The Drygalski Ice Tongue extended as far east as 165.5°E in May 1998. The excursion into TNB began on May 25 (day 145) at 75°S, 175°E. Late morning on May 27 (UT, day 147) we reached 74.915°S, 163.833°E, a point 1.852 km (1 nautical mile) from the front of the Hells Gate Ice Shelf on the Victoria Land coast (Figure 1). From there we proceeded to 75.332°S, 164.688°E near the northern edge of the Drygalski Ice Tongue before crossing the entire width of TNB to Cape Washington (Figure 1), which was reached midmorning on May 28 (UT, day 148). We left Cape Washington early morning on May 29 (day 149), and the TNB excursion ended on May 31 (day 151) at 74.783°S, 175°W.

3. Methods

3.1. Ice Observation Method

A program of standardized ice observations was maintained while the ship was underway in the pack ice. The ice observation program [*Worby and Allison,* 1999] is endorsed by the Scientific Committee for Antarctic Research (SCAR) as the standard for ship-based acquisition of Antarctic sea ice data. Ice observations were made each hour from the ship's bridge. For each observation the ice cover was divided into three thickness categories, and for each category the concentration, mean unridged ice thickness, mean snow depth on the unridged ice, and areal extent and height of ridges were estimated. A simple empirical ridge profile model [*Worby et al.,* 1998] calculates the mean ridged ice thickness from ridge extent and height data. The calculation of the mean ridged ice thickness does not include the use of a ridge height cutoff because that would exclude a large volume of ice below the waterline [*Worby et al.,* 1996; K. Morris, M. O. Jeffries, T. Tin, and N. Kozlenko, Late autumn ice concentration, thickness and ridging distributions in the Ross Sea, submitted to *Journal of Glaciology,* 2000, hereinafter referred to as Morris et al., submitted manuscript, 2000].

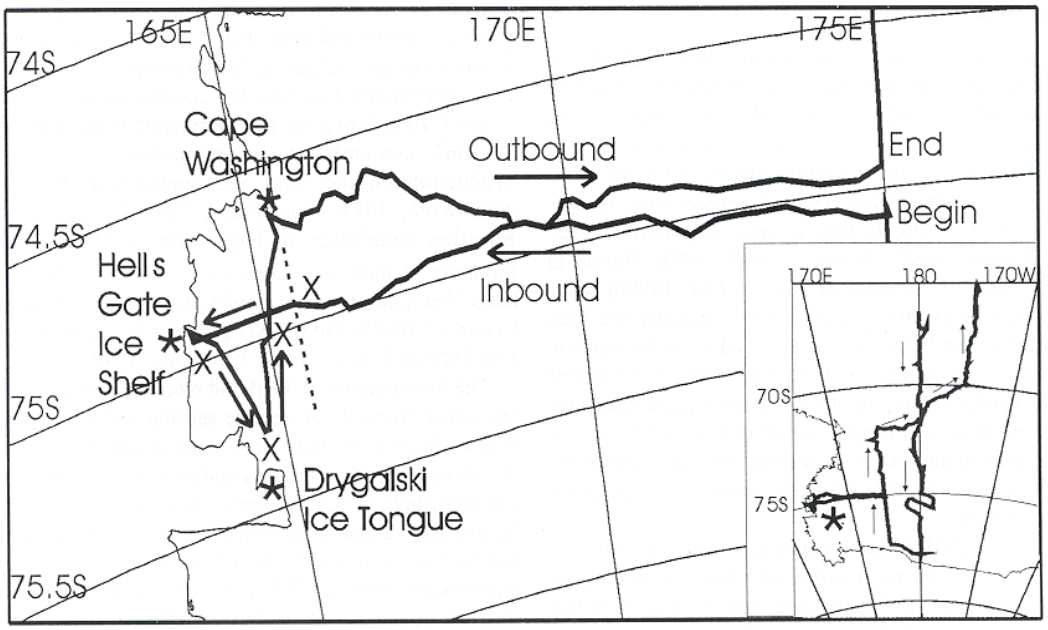

Figure 1. Map of the inbound and outbound tracks of the R/V *Nathaniel B. Palmer* during the excursion into and out of TNB between May 25 (day 145) and May 31, (day 151) 1998. The tracks were almost coincident between longitudes 169° and 169.5°E, but otherwise, the outbound leg always lay to the north of the inbound leg. Prior to and after this excursion the ship's track was northbound along the 175°E meridian. The insert shows the ship's track for the entire Ross Sea cruise in May and June 1998, including the TNB inbound and outbound legs, which are identified by the asterisk. Drygalski Ice Tongue extended to 165.5°E in May 1998, defining the eastern edge of TNB (dashed line). The locations of samples obtained for ice texture analysis are identified by a cross.

The mean unridged ice and mean ridged ice thickness values are added to give a mean effective ice thickness. Each of these values is calculated over the entire pack ice, including the open water fraction, i.e., for a unit area. The advantage of this approach is that ice thickness values calculated from these standardized observations can be compared directly regardless of time and location. Since there were only two observations of <10/10 ice cover (west of 164°E in westernmost TNB), there is negligible difference between the mean ice thickness values calculated over the unit area and those calculated over the fractional ice area.

The estimates of the unridged ice thickness variability are based on observations of floes that turn on edge along the side of the ship below a float of 0.4 m diameter. *Worby* [1998] suggests that the uncertainty in the unridged ice thickness estimates is ±20% for thin ice, i.e., ice <0.3 m thick, and ±10% for thicker ice. Uncertainties in the estimates of the areal extent of ridging have not been quantified. While we recognize that accurate estimates of ridging extent are difficult, uncertainties in those estimates and in the unridged ice thickness estimates are reduced by the large number of observations that are made and then binned into broad-area averages.

For the purpose of data presentation we define an inbound leg, an outbound leg, and a grouped TNB leg. The inbound leg is from 175°E to Hells Gate Ice Shelf, and the outbound leg is from Cape Washington to 175°E (Figure 1). Along both these legs the data have been binned at 1° longitude intervals, with 175°E as the reference datum. The grouped TNB leg combines all the observations from (1) the point of entry at longitude 165.5°E to Hells Gate Ice Shelf, (2) Hells Gate Ice Shelf to Drygalski Ice Tongue, and (3) Drygalski Ice Tongue to Cape Washington (Figure 1). The grouped TNB ice data are binned at 0.5° longitude intervals, with 164°E as the reference datum. Binning the data creates a "snapshot" summary of the observations and is a practical method of analyzing a short duration data set.

3.2. Satellite-Derived Ice Concentration/Open Water

To assess the representativeness of the ship-based ice observations and derived fluxes in TNB, ice concentration (C in percent) data for the period March 21 to June 21, 1998, were obtained from the National Snow and Ice Data Center (NSIDC). To place the 1998 data in a longer term perspective, ice concentration during the period May 21-31, 1998, is compared with that during May 21-31 each year from 1988-1998. The period May 21-31 was chosen for convenience because it covered a full week of ice cover variability prior to the in situ observations in TNB on May 28 and terminated with the end of the outbound leg on May 31. The NSIDC ice concentration data are derived from SSM/I satellite passive microwave brightness temperatures using the NASA Team algorithm [*Cavalieri et al.*, 1994] and mapped to a polar stereographic grid [*NSIDC*, 1996]. The open water fraction is calculated from the ice concentration, i.e., 100 - C.

Sources of error in the SSM/I-derived ice concentration data relate to (1) the difficulty in distinguishing open water and new ice from low concentrations of thick ice, compounded by mixing effects due to the presence of various ice types within the large (25 x 25 km) pixels, and (2) contamination of coastal pixels by the adjoining ice sheet/land, although this effect is minimal for larger polynyas [*Massom et al.*, 1998a]. More accurate estimates of ice concentration/open water in coastal areas can be obtained using the higher-resolution 85 GHz channels [*Markus and Burns*, 1995], but the data set for 1988-1998 is incomplete. Ice concentration may be over-estimated in large polynyas because of the effects of wind roughening of open water on emissivity [*Steffen and Schweiger*, 1991].

Despite unavoidable errors, passive microwave data can be used with confidence because they effectively illustrate temporal changes in coastal polynya extent and, in the case of TNB, much of the variation in derived open water/ice concentration represents real changes [*Van Woert et al.*, 1992; *Van Woert*, 1999b]. For this study, errors in the absolute values are not a significant issue as we are primarily interested in the state of the ice in TNB on a relative basis and are using the satellite-derived values for comparative purposes.

3.3. Air temperature and wind speed

Air temperature, wind speed and direction, and humidity were recorded automatically at 1 min intervals aboard the R/V *Nathaniel B. Palmer*. Hourly data have been extracted from the raw data to illustrate the weather conditions during the TNB excursion. They provide a background to the environment in which the sea ice observations were made, and they illustrate some of the inputs to the heat flux calculations.

To place the ship-based air temperature and wind speed in TNB in perspective, we analyzed data obtained at 10 min intervals at AWS 8905 at 74.95°S, 163.69°E on Inexpressible Island, only 8.5 km from the westernmost point reached by the ship offshore from Hells Gate Ice Shelf. Mean daily temperatures and wind speeds for the period May 21-31 each year from 1988 to 1998 were calculated from AWS data recorded at 0, 3, 6, 9, 12, 15, 18 and 21 hours each day. Occasionally, data were not recorded on the hour. In those cases the nearest available data point was used and it was typically within ±1 hour of the reference time. The AWS 8905 temperature record is complete for each year, but wind data are missing in some years, including 1998, because of anemometer malfunctions.

3.4. Heat flux calculations

Estimates of the instantaneous conductive heat flux (F_c in W m^{-2}) through the ice and snow cover were calculated according to

$$F_c = \frac{T_s - T_f}{\left(\frac{H_i}{k_i} + \frac{H_s}{k_s}\right)}, \quad (1)$$

here T_s is the snow surface temperature, T_f is the ocean temperature (-1.84°C, the freezing point of seawater with a salinity of 34.5, as described below), H_s and H_i are the snow and ice thicknesses, respectively, and k_s and k_i are the snow and ice thermal conductivities, respectively. The assumptions behind this approach have been discussed at length elsewhere, and it has been shown that it provides satisfactory flux estimates [*Sturm et al.*, 1998; *Jeffries et al.*, 1999].

For k_s we use two different values: 0.14 and 0.31 W m^{-1} K^{-1}. The higher k_s value is typically used in numerical models of sea ice and climate [*Massom et al.*, 1998b; *Wu et al.*, 1999]. The lower k_s value is calculated according to *Sturm et al.* [1997] from the mean snow density (315 kg m^{-3} and n = 161) in 42 snowpits on 20 different floes throughout the western Ross Sea in May and June 1998 [*Morris and Jeffries*, 2001]. Similar low k_s values have been reported at other times of year and elsewhere on Antarctic sea ice [*Massom et al.*, 1997, 1998b; *Sturm et al.*, 1998]. For k_i we follow *Cox and Weeks* [1988], with the ice salinity (per mil) estimated according to *Kovacs* [1996]:

$$S = 4.644 + \frac{0.8666}{H_i}. \quad (2)$$

The snow surface temperature is computed from the surface energy balance:

$$F_l + F_E + F_s + F_e + F_c = 0, \quad (3)$$

where F_l is the incoming long-wave radiation, F_E is the emitted long-wave radiation, F_s and F_e are the sensible and latent heat fluxes, respectively, and F_c is the conductive heat flux. Short-wave fluxes are omitted since they are near zero in TNB at this time of year. F_l is estimated according to *König-Langlo and Augstein* [1994]:

$$F_l = \sigma T_a^4 (0.765 + 0.22C^3), \quad (4)$$

and F_E is estimated according to

$$F_E = -\varepsilon \sigma T_s^4, \quad (5)$$

where T_a and T_s are air and surface temperature, respectively, σ is the Stefan-Boltzmann constant, ε is the emissivity with a value of 0.98, and C is the relative cloud cover. The turbulent fluxes are given by [*Cox and Weeks*, 1988]

$$F_s = \rho_a c_p C_H u (T_a - T_s) \quad (6)$$

$$F_e = \rho_a L C_E u (q_a - q_s), \quad (7)$$

where ρ_a is the air density, c_p is the specific heat, u is the wind speed, L is the latent heat of vaporization, and q_a and q_s are the specific humidities of the air at the reference level and the surface, respectively. C_H and C_E are the transfer coefficients, defined at a specific reference level. As there are few good measurements of the transfer coefficients, we follow the Reynolds analogy and assume they are both equal to the surface drag coefficient. For the latter we use a value of 1.5 x 10^{-3}, typical of low roughness ice in the Weddell Sea [*Wamser and Martinson,* 1993]. This is equivalent to a value of 1.2 x 10^{-3} at the reference height of 30 m on the R/V *Nathaniel B. Palmer,* according to the flux gradient method [*Andreas and Murphy,* 1986] and the theory of *Andreas* [1987] for the conditions encountered in TNB. Given that snow and ice surface temperatures will be close to the air temperature, the actual transfer coefficients should be quite close to the neutrally stable value.

For the ice-covered area of TNB and the pack ice, mean relative humidity, mean wind speed and mean air temperature values for each longitudinal bin were calculated from the ship's meteorological record and, together with a cloud cover value of 1 (100%), were used as inputs to the flux calculations. The cloud cover value is based on visual assessment of National Oceanographic and Atmospheric Administration (NOAA) advanced very high resolution radiometer (AVHRR) satellite images for the period of the TNB excursion. For the open water adjacent to Hells Gate Ice Shelf the heat flux was calculated explicitly for ice growth at an open water surface on the basis of the assumptions of *Kurtz and Bromwich* [1985], with air

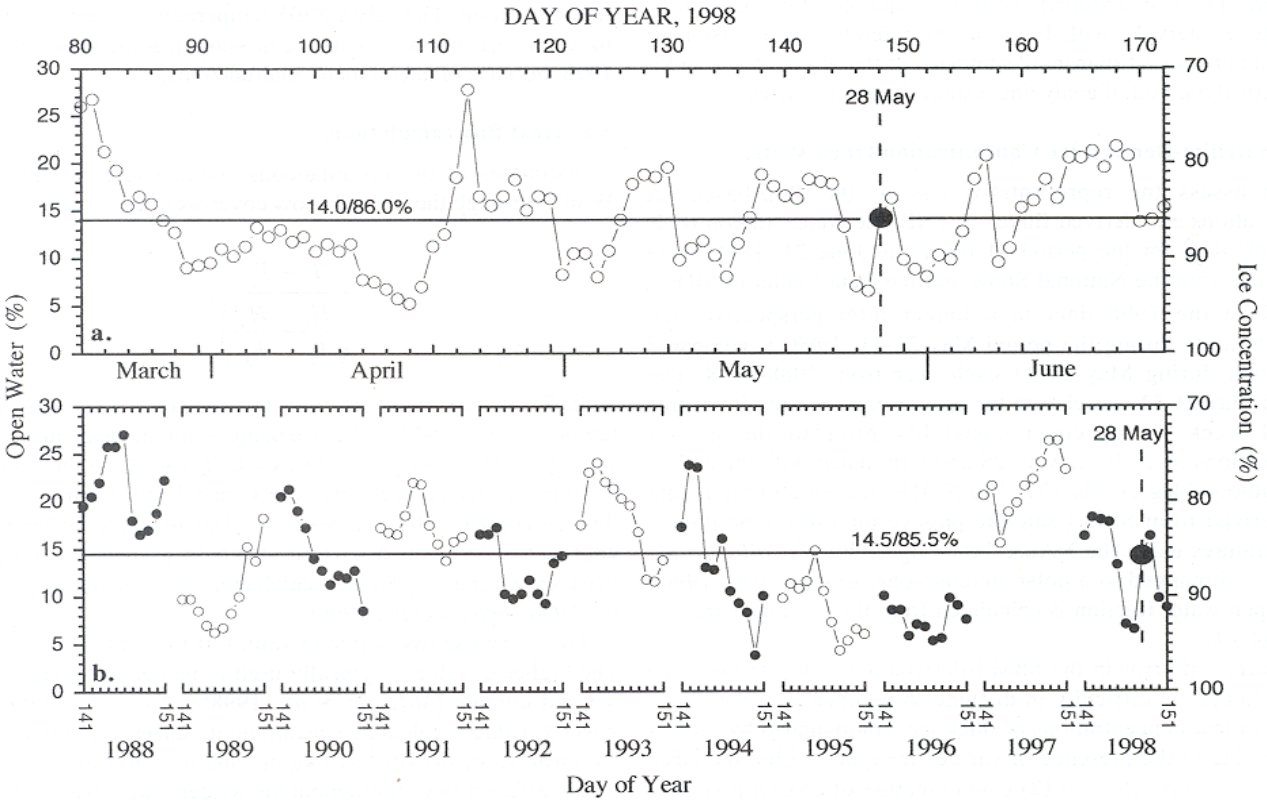

Figure 2. Temporal variability of daily open water/ice concentration in TNB during (a) autumn 1998 and (b) the period May 21-3 (days 141-151) each year from 1988 to 1998, as determined from SSM/I satellite passive microwave data. The solid horizontal lines represent mean open water/ice concentration values. The vertical dashed line and the large solid circle on May 28 identify when the snow and ice observations were made in TNB.

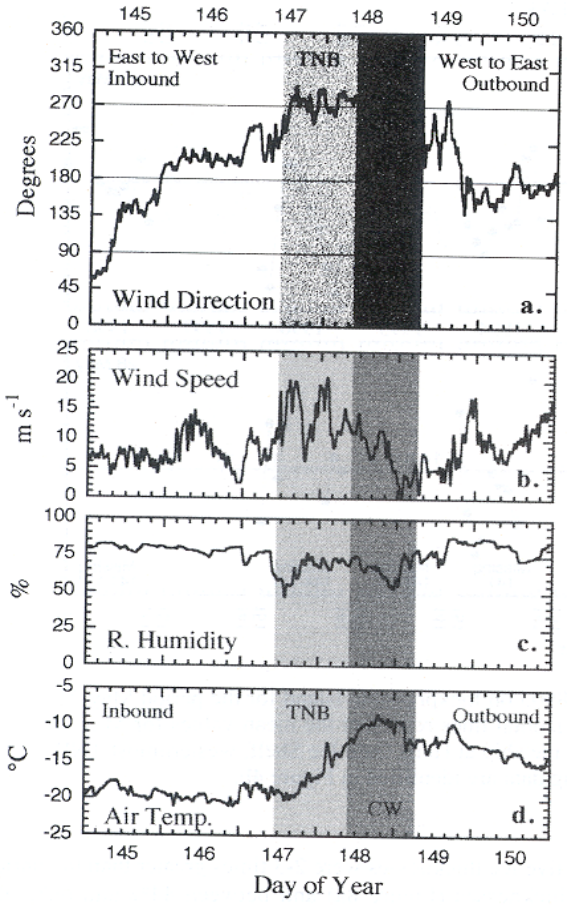

Figure 3. Hourly (UT) variation of (a) wind direction, (b) wind speed, (c) relative humidity, and (d) air temperature from day 145 to day 150, i.e., from the beginning of the inbound leg as far as Hells Gate Ice Shelf, Hells Gate Ice Shelf to Cape Washington (CW), and CW to the end of the outbound leg. The lightly shaded area identifies the period when ice observations were made in TNB. The darker shaded area identifies the period when the ship was stationary at CW.

temperature, wind speed, and humidity inputs of –19.8°C, 17.0 m s^{-1}, and 57.5%, respectively, as recorded aboard the ship at that location.

4. Results

4.1. Variability of the Autumn Ice Cover in TNB, 1988-1999

SSM/I-derived sea ice concentration charts for the period May 21-31, 1998, in the southwestern Ross Sea, including TNB, are shown in Plate 1. Changes in ice concentration as the polynya opened and closed can be seen, and it appears that the state of the polynya was related to whether or not a band of 100% concentration ice extended into the southwesternmost Ross Sea. This phenomenon, observed in electrically scanning microwave radiometer (ESMR) and scanning multichannel microwave radiometer (SMMR) satellite passive microwave data [*Sturman and Anderson,* 1986; *Jacobs and Comiso,* 1989] and suggested as an influence on the state of the TNB polynya [*Van Woert,* 1999b], will be discussed.

The SSM/I-derived variability of open water and ice concentration in TNB in autumn 1998 is shown in Figure 2a. The area of open water varied between 5.25 and 27.75%, with a mean value of 14.0%. On May 28, when the snow depth and ice thickness observations were made in the bay, the polynya was undergoing a brief opening, and the area of open water was 14.25%. Thus the state of TNB and the ice cover (85.75% concentration) on May 28 were normal with respect to autumn 1998 as a whole.

The variability of open water and ice concentration in TNB during the interval May 21-31 from 1988 to 1998 is shown in Figure 2b. During this 11 day interval over a period of 11 years the area of open water varied between 3.75 and 27.0%, with a mean value of 14.5%. Thus, the state of the ice cover on May 28, 1998, in TNB also was normal with respect to the decadal record for late May.

4.2. Weather Conditions in May 1998

A key feature of the weather, as recorded aboard the ship, was the persistent westerly wind in TNB (Figure 3a), which apart from a brief lull toward the end of day 147 (Figure 3b) near the Drygalski Ice Tongue, was stronger (peak speeds of 20 m s^{-1}) than the easterly to southerly wind that was more typical of the region outside the bay. Minimum relative humidity values occurred in TNB (Figure 3c). The occurrence of a strong, dry westerly wind in the bay is consistent with the katabatic air flow off the continent that plays a key role in polynya activity [*Kurtz and Bromwich,* 1983, 1985; *Bromwich and Kurtz,* 1984]. As we proceeded farther into the bay along the inbound leg, air temperature increased (Figure 3d), which is consistent with previous observations that the surface temperature within the katabatic flow can be warmer than at the surface outside the flow [*Parish and Bromwich,* 1989]. The westerly wind continued but declined in speed until shortly before we left Cape Washington, when it was almost calm (Figure 3b) and veered to the north (Figure 3a).

The mean daily air temperature and wind speed at AWS 8905 on Inexpressible Island for the period May 21-31 from 1988 to 1998 are presented in Figure 4. The end of May 1998 was warmer than it had been in most previous years: the mean temperature during May 21-31, 1998, was –23.6°C compared to –26.8°C for the same 11 day period during 1988-1998. The mean daily temperature on May 28, 1998, was –19.4°C compared to the mean of –24.9°C for the same day during 1988-1998. AWS wind data are unavailable for 1998, but during the 50 min that the R/V *Nathaniel B. Palmer* was at its westernmost location and holding station for ice sampling close to the Hells Gate Ice Shelf and AWS 8905, the mean wind speed aboard the ship was 17.0 m s^{-1}, i.e., higher than the mean wind speed of 14.8 m s^{-1} on May 28 from 1988 to 1997.

4.3. Sea Ice Thickness Variability in May 1998

4.3.1. Unridged ice thickness and snow depth variability. TNB was almost entirely covered with ice and the 6% areal coverage of open water (Figure 5a) occurred in the western extremity of the bay immediately offshore from Hells Gate Ice Shelf. Considering the differences in technique, there is good agreement between the ship-based observations and the SSM/I-derived open water/ice concentration of 14.25% (Figure 2).

In the open water at the front of the Hells Gate Ice Shelf a significant amount of frazil ice was being formed, and it was being transformed quickly into pancakes. They, in turn, were rapidly consolidating into sheet ice over distances of a few hundreds of meters. Almost all of the ice cover in TNB was sheet

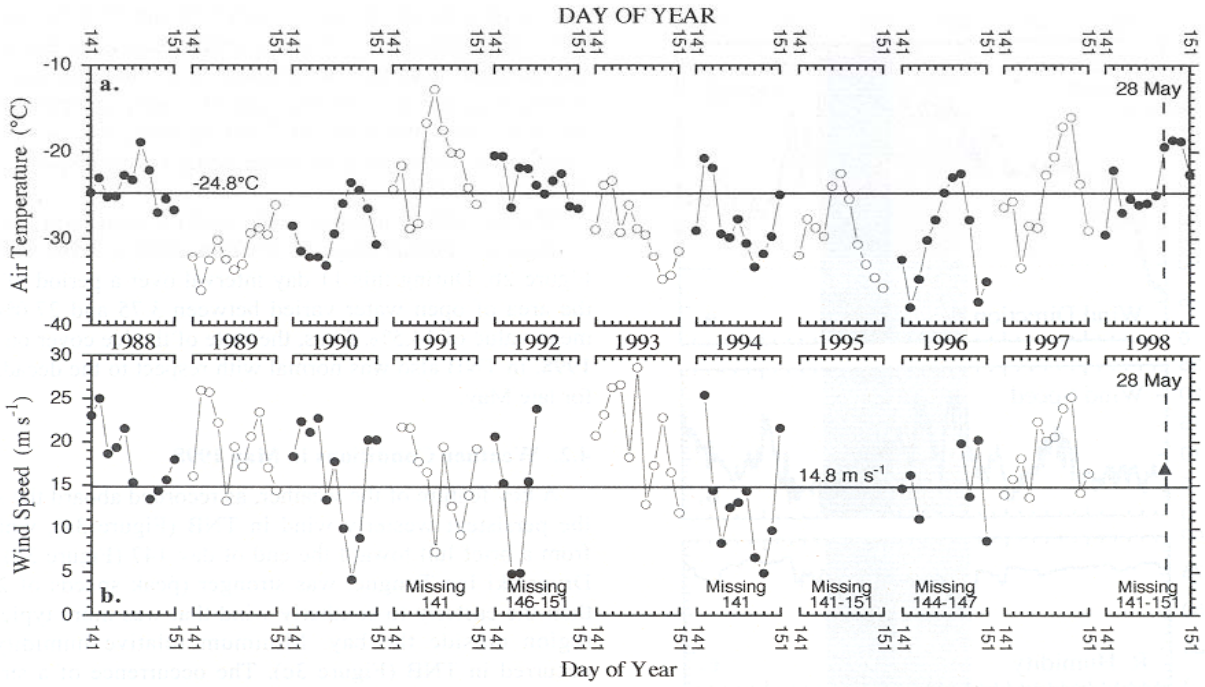

Figure 4. Mean daily air temperature and wind speed at AWS 8905 on Inexpressible Island for the period May 21-31 (days 141-151) each year from 1988 to 1998. The solid horizontal lines represent the mean values for May 28 during the period 1988-1998. The wind speed measured aboard the ship at Hells Gate Ice Shelf, westernmost TNB, is shown as a triangle in the lower right graph. Days with missing data are identified in Figure 4b.

ice. Of the unridged sheet ice cover, 87% was ≤0.3 m thick (Figure 5a). Textural and stable isotopic analysis of thin ice samples taken in and immediately outside the bay (Figure 1) showed that the sheet ice was composed almost entirely of consolidated granular frazil ice. Only 2.8% of the granular ice was snow ice.

There was a pronounced ice thickness gradient within TNB, with a fivefold increase in unridged ice thickness (0.05-0.25 m) from west to east (Figure 5b). There was also a west-east increase in snow depth, from 0 to 0.03 m (Figure 5b), with snow depth/ice thickness ratios (S/I) of 0-0.12. The thin snow cover and the low snow/ice thickness ratios account for the very small amount of snow ice observed in the ice samples.

The spatial variability of the unridged ice thickness along the inbound and outbound legs is shown in Figure 6. The pattern was essentially the same along each leg, with an ice thickness maximum located roughly midway between the ice thickness minima at the beginning and end of each leg. Combined, the two legs have a broad ice thickness maximum of 0.6 to 0.7 m between 169° and 172°E. On the inbound leg there was a tenfold decrease in ice thickness from the maximum (0.6 m) at 171°-172°E to the minimum (0.06 m) at 164°-164.5°E, the most westerly section of TNB. A similar pronounced ice thickness gradient was not observed in the data for the outbound leg as it began at the outer, northeastern margin of the bay. Maximum snow depths (0.07-0.09 m) occurred in the region of maximum ice thickness (Figure 6), but like those in the bay, were only a small fraction of the total thickness of snow plus ice, with S/I ratios of 0.11-0.15.

4.3.2. Areal extent of ridging and effective ice thickness variability. The sheet ice in TNB was being thickened dynamically by ridging, which varied between 2.5 and 18.5% in areal extent (Figure 7a). As a consequence of the ridging, the effective ice thicknesses were 2-3 times greater than the unridged ice thicknesses (Figure 8a) and between 44% and 66% of the total ice mass was contained within the 2.5-18.5% of the TNB ice cover that was ridged (Figure 7a). The areal extent of ridging, effective ice thickness, and contribution of ridges to the total ice mass within the polynya each showed a strong gradient as a function of distance from shore (Figures 7a and 8a).

On the inbound and outbound legs the areal extent of ridging in the pack ice varied between 5 and 35%, and 9 and 30%, respectively, with the least ridging at the beginning and end of each leg (Figures 7b and 7c). Factoring in the contribution of the ridges to the ice thickness distribution leads to effective ice thicknesses 1.5-3 times greater than the unridged ice thicknesses (Figures 8b and 8c). Between 30% and 60% of the total ice mass was contained within the 5-35% of the pack ice that was ridged (Figures 7b and 7c).

4.4. Heat Flux

The heat flux was calculated for the unridged ice and for the effective ice thickness in each of the 1° longitudinal bins along the inbound and outbound legs and the 0.5° longitudinal bins in TNB using the two different bulk snow thermal conductivity values. In this way we can illustrate the potential variability of the heat flux. To investigate the degree to which the flux estimates in TNB were a function of the fact that May 28, 1998, was 5.5°C warmer than the mean temperature for that day during 1988-1999, the fluxes were also calculated using air temperatures 5.5°C lower than those recorded aboard the ship and assuming the same snow and ice thickness.

Regardless of the choice of k_s and the fact that the air temperature on May 28, 1998, was 5.5°C higher than the long-term average, the area-weighted mean heat fluxes in TNB (open

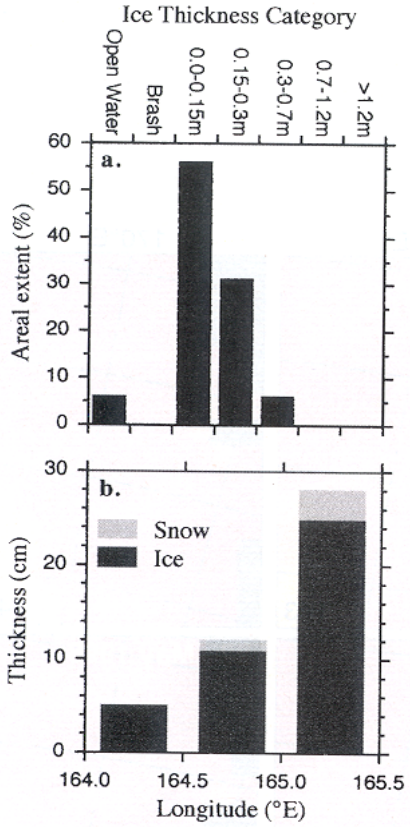

Figure 5. (a) Areal extent of open water and different ice thickness categories (World Meteorological Organization sea ice nomenclature) in TNB. (b) Mean snow depth and mean thickness of unridged ice in 0.5° longitude wide bins in TNB (the snow depth is shown as a cumulative addition to the ice thickness). These data are a summary of all observations made along the three cruise legs in TNB (see Figure 1).

water and ice) were an order of magnitude greater than those in the pack ice (Table 1). The spatial variability of heat flux in TNB and in the pack ice is presented in Figures 9 and 10, respectively. For the observed air temperature, wind speed and humidity at Hells Gate Ice Shelf the heat flux from the open water was 764 W m^{-2} (Figure 9a). Adjusting the air temperature by -5.5°C increased the heat flux from the open water by 25% to 958 W m^{-2} (Figure 9b). Between westernmost and easternmost TNB the heat flux decreased by an order of magnitude as the ice and snow thickness increased (Figure 9). The heat flux at the eastern edge of TNB was slightly higher than, but of the same order of magnitude as, the fluxes in the pack ice (Figures 9 and 10).

For the pack ice and for the ice covered area of TNB the fluxes were higher for the unridged ice than for the effective ice thickness and higher for the low k_s value than for the high k_s value, as one would expect (Figures 9 and 10). In the pack ice the heat flux varied according to the ice thickness variations on each leg, and the flux on the outbound leg was slightly lower than that on the inbound leg because of the higher air temperatures (Figure 3d) and generally thicker ice (Figures 6 and 8).

5. Discussion

5.1. Sea Ice Cover

The spatial variability of the unridged ice thickness observed on the inbound and outbound legs, particularly the decrease in ice thickness toward the coast, is not unusual in the Antarctic pack ice. It is a more localized version of an ice edge-to-continent pattern observed in the East Antarctic pack ice [*Allison and Worby,* 1994] and in the western Ross Sea [*Jeffries and Adolphs,* 1997; Morris et al., submitted manuscript, 2000]. The unridged ice thickness values, snow depth values, and snow/ice ratios along the inbound and outbound legs are each similar to those observed in the Ross Sea pack ice between the ice edge and the Ross Ice Shelf in autumn 1998 (Morris et al., submitted manuscript, 2000). On the other hand, the maximum values for areal extent of ridging and the contribution of ridges to the total ice mass along both the inbound and outbound legs exceed those observed between the ice edge and the Ross Ice Shelf in autumn 1998 (Morris et al., submitted manuscript, 2000).

The region of the inbound and outbound legs is one that has previously been found to be the most heavily ridged in airborne laser profiles of the Ross Sea ice cover [*Weeks et al.,* 1989]. It is a region that coincides with a zone of cold, thick ice observed flowing northeastward from the southwesternmost Ross Sea in satellite thermal infrared images [*Szekielda,* 1974; *Kurtz and Bromwich,* 1983, 1985]. A thick ice band in this region has been reproduced in numerical simulations of the TNB polynya and adjacent pack ice [*Gallée,* 1997, Figure 7].

The high concentration ice band can be seen in Plate 1. It is also a transient feature: the ice concentration fluctuates, and the ice band appears to undergo a cycle of advance and retreat. This has previously been reported by *Van Woert* [1999a, 1999b], who noted that the mechanism responsible for the breakdown of the compact ice band is not well understood. Regardless of its cause, the cycle of opening and closing of the pack ice in this region will promote new ice formation on the one hand and dynamic

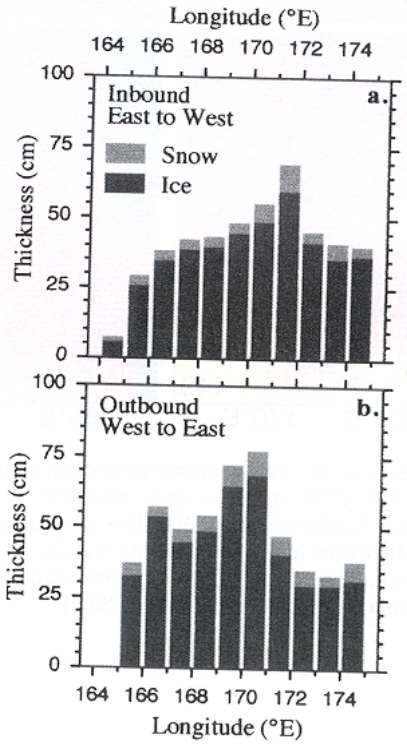

Figure 6. Mean snow depth and mean thickness of unridged ice in 1° longitude wide bins along (a) the inbound leg to TNB and (b) the outbound leg from TNB. The snow depth is shown as a cumulative addition to the ice thickness.

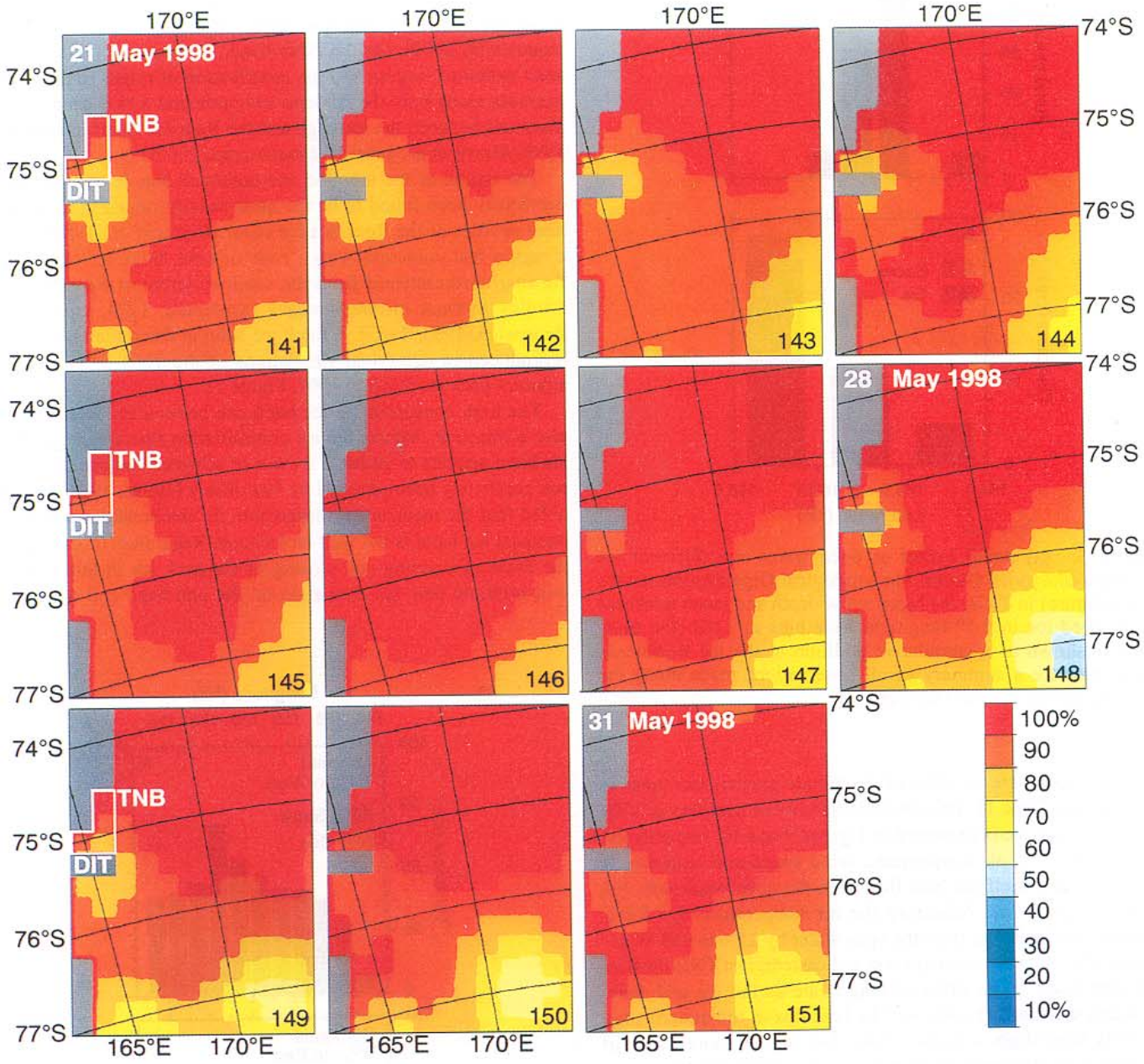

Plate 1. Polar stereographic projection charts of SSM/I-derived ice concentration for the period May 21-31, (days 141-151) 1998, in the southwestern Ross Sea. The day of year is given in the lower right corner. The Drygalski Ice Tongue is identified by DIT. The grey areas at the left of each chart are continental pixels. The reversed L-shaped box in white identifies the four pixels for which the area-weighted ice concentration/open water in TNB were derived. The region of low ice concentration in the lower right corner, for example, days 148-150, is the Ross Sea polynya adjacent to the Ross Ice Shelf.

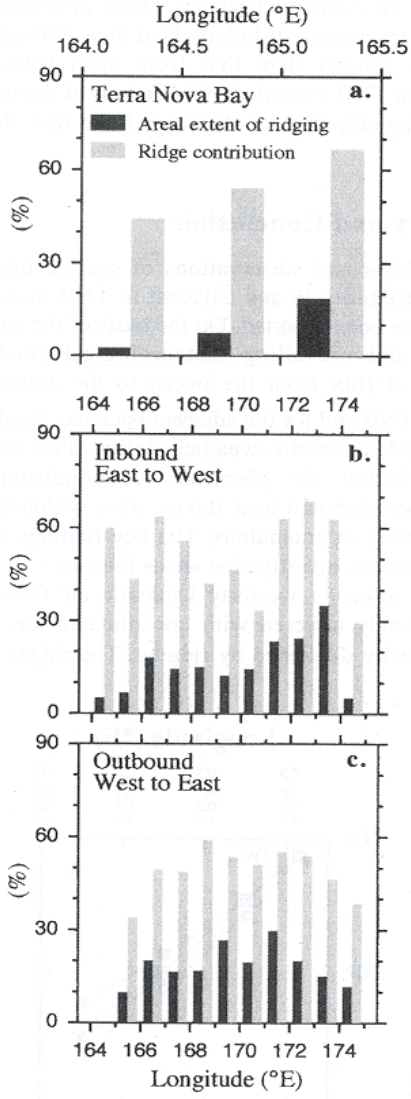

Figure 7. Areal extent of ridging and the contribution of ridges to the total ice mass (a) within TNB, (b) along the inbound leg to TNB, and (c) along the outbound leg from TNB. The binning increment is 0.5° of longitude in Figure 7a and 1° in Figures 7b and 7c.

thickening by ridging on the other, leading to the extensive ridging and significant contribution of ridges to the ice thickness and ice mass observed on the inbound and outbound legs. Ridging in this region is probably also promoted as ice moving eastward away from Victoria Land under the influence of the katabatic wind [*Jacobs and Comiso,* 1989], which extends as much as 200 km offshore of TNB [*Kurtz and Bromwich,* 1985], interacts with the ice flowing northeastward from the southwesternmost Ross Sea.

During the 3 days of the inbound leg prior to the observations in TNB the high concentration ice band extended further south and covered a much larger area (Plate 1, days 145-147) than it did during the rest of the period May 21-31 (Plate 1) and minimum open water occurred in the bay (Plate 1). On the day the observations were made in TNB, there was a slight increase in the amount of open water in the bay (Figure 2) as the high concentration ice band began to recede (Plate 1, day 148). It is likely that the extensive, ridged ice cover observed in TNB on May 28 was the culmination of the blocking effect of the high concentration, thick, ridged sea ice band during days 145-148, when it acted as a barrier that prevented the export of newly formed ice from TNB. Under those circumstances the ice in the bay would not have been in free drift (a basic assumption of polynya models); consequently, it consolidated and ridged rather than being advected farther east in response to the strong westerly winds. The in situ and remotely sensed observations of the state of the ice cover in and adjacent to TNB provide corroborating evidence for the suggestion [*Van Woert,* 1999a, 1999b] that the development of the TNB polynya is influenced not only by the local katabatic winds and air temperatures but also by the compactness of the sea ice in the southwestern Ross Sea.

That there was an extensive and relatively thick and ridged sheet ice cover in TNB was not a complete surprise. In May 1995 and May 1998 we also observed negligible open water and extensive rafting of nilas and young ice in the Ross Sea polynya immediately north of the Ross Ice Shelf [*Jeffries and Adolphs,* 1997; Morris et al., submitted manuscript, 2000]. Extensive

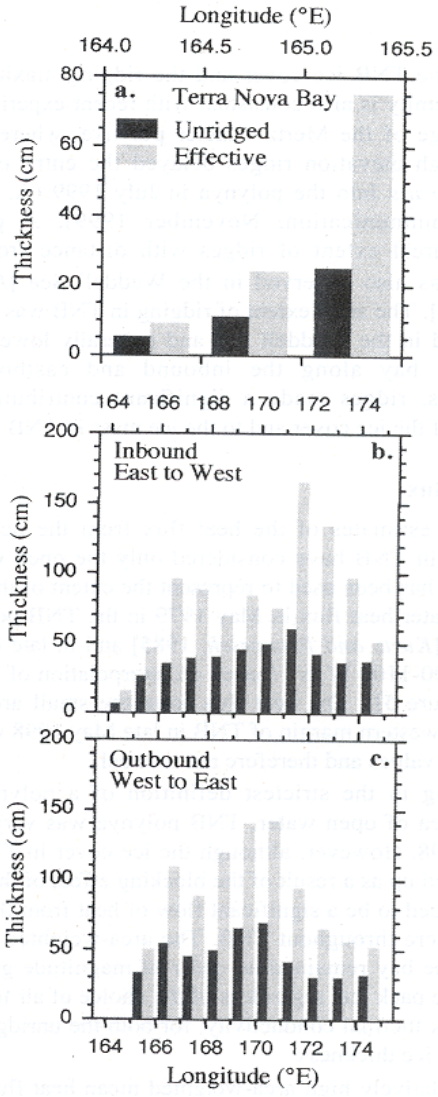

Figure 8. Mean thickness of unridged ice and mean effective ice thickness (a) within TNB, (b) along the inbound leg to TNB, and (c) along the outbound leg from TNB. The binning increment is 0.5° in Figure 8a and 1° of longitude in Figures 8b and 8c.

Table 1. Area-Weighted Mean Conductive Heat Fluxes in TNB and in the Pack Ice During the Inbound and Outbound Legs, May 25-31, 1998.

	TNB (Observed T, °C)	TNB (Observed T-5.5, °C)	Pack Ice, Inbound	Pack Ice, Outbound
Unridged ice, k_s: 0.14 W m^{-1} K^{-1}	199 (23%)	246	35	20
Effective ice thickness, k_s: 0.14 W m^{-1} K^{-1}	156 (30%)	191	24	15
Unridged ice, k_s: 0.31 W m^{-1} K^{-1}	216 (21%)	268	49	30
Effective ice thickness, k_s: 0.31 W m^{-1} K^{-1}	164 (28%)	201	31	20

Note: the heat flux in TNB was calculated at the observed air temperatures (T) (column 2) and at T-5.5°C (column 3) to allow for the fact that T on 28 May, 1998, was 5.5°C higher than the mean T for May 28 from 1988 to 1998. The values in parentheses in column 2 represent the proportion of the heat flux from the open water.

ridging of the TNB ice cover and the ridging maximum at its eastern extremity is also consistent with recent experience at the northern edge of the Mertz Glacier polynya, where extensive fields of high elevation ridges delayed the entry of the R/V *Aurora Australis* into the polynya in July 1999 (A. P. Worby, personal communication, November 1999). A pattern of increasing areal extent of ridges with distance from coastal polynyas was also observed in the Weddell Sea [*Eicken and Lange,* 1989]. The areal extent of ridging in TNB was lower than that reported in the Weddell Sea and generally lower than that outside the bay along the inbound and eastbound legs. Nevertheless, ridges made a significant contribution to the thickening of the ice cover and to the ice mass in TNB.

5.2. Heat Flux

Previous estimates of the heat flux from the ocean to the atmosphere in TNB have considered only the open water area, which alone has been used to represent the extent of the polynya. The open water heat flux in May 1979 in the TNB polynya was 814 W m^{-2} [*Kurtz and Bromwich,* 1985] and in late May 1988-1990 was 800-1100 W m^{-2} (based on interpolation of *Van Woert* [1995b, Figure 5]). The heat flux from the small area of open water at the western margin of TNB in late May 1998 was similar to the above values and therefore not unusual.

According to the strictest definition of a polynya, i.e., a recurrent area of open water, TNB polynya was very small on May 28, 1998. However, although the ice cover in TNB had, in effect, backed up as a result of the blocking effect of the pack ice, there continued to be a significant flow of heat from the ocean to the atmosphere throughout TNB. The area-weighted mean heat flux from the bay remained an order of magnitude greater than that from the pack ice, regardless of the choice of air temperature or snow bulk thermal conductivity, for both the unridged ice and the effective ice thickness.

Of the relatively high area-weighted mean heat flux in TNB, no more than 30% was from the open water (Table 1); the greatest proportion of the heat loss occurred through the ice. *Worby and Allison* [1991] reported a similar phenomenon in simulations of turbulent fluxes over the thin, variable concentration East Antarctic pack ice. There, at concentrations of 80-100% the fractional turbulent heat loss through thin ice (<0.3 m) was greater than that from open water. The ice concentration in TNB exceeded 90%, and all of the unridged ice and much of the effective ice thickness there was <0.3 m thick (Figure 8a).

6. Summary and Conclusion

The first ship-based observations of sea ice thickness and snow depth variability in and adjacent to TNB in autumn (late May 1998) have been reported. On the basis of the snow and ice observations and prevailing meteorological conditions the conductive heat flux from the ocean to the atmosphere was estimated for TNB and for the adjacent pack ice. Satellite passive microwave and automatic weather station data were used to determine whether the observed ice conditions, and by implication the estimated heat fluxes, were within the limits of normal variability or anomalous. The key findings of this TNB sea ice and heat flux investigation are as follows:

1. Despite a strong westerly katabatic air flow, TNB was almost completely covered with consolidated ice, which was being dynamically thickened by ridging. The ridges contributed

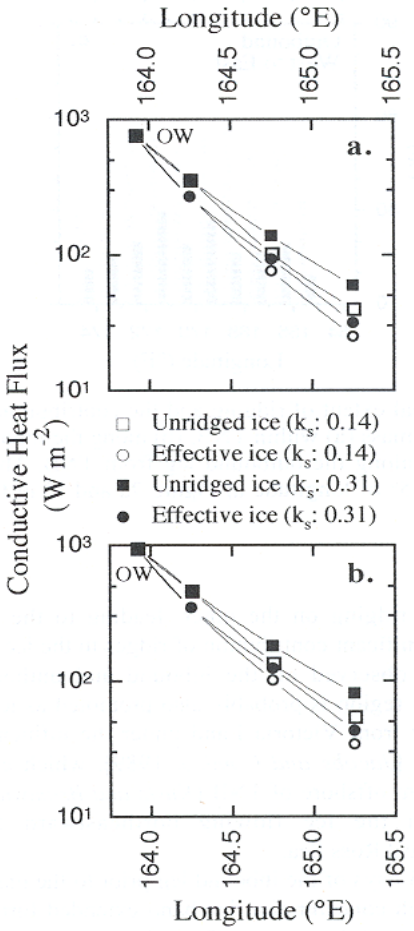

Figure 9. Conductive heat flux variability for the open water (OW) and for the unridged and effective ice thicknesses in the 0.5° longitude wide bins in TNB for (a) observed temperatures and (b) observed temperatures minus 5.5°C. For the ice-covered bins the heat flux is shown as a function of snow bulk thermal conductivity k_S. A common log scale is used to expand the scale and increase the spacing between symbols.

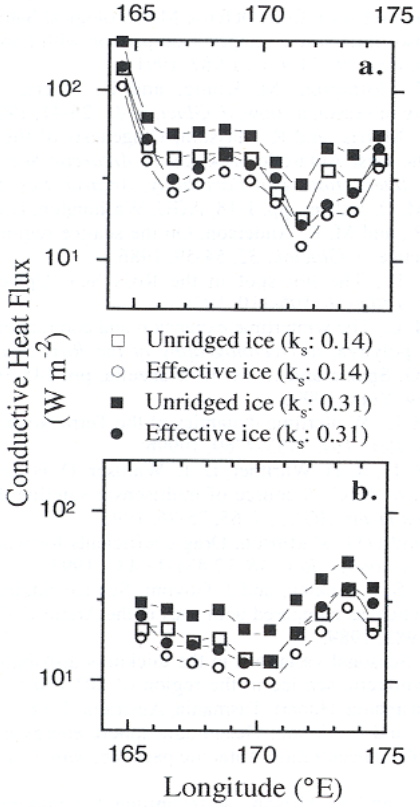

Figure 10. Conductive heat flux for the unridged and effective ice thicknesses in the 1° longitude wide bins along (a) the inbound leg to TNB and (b) the outbound leg from TNB as a function of snow bulk thermal conductivity k_S. The highest flux values for the open water in westernmost TNB (see Figure 9) have been omitted deliberately, and a common log scale is used, resulting in an expanded scale that increases the spacing between symbols.

as great a proportion to the ice mass in the bay as they did to the pack ice outside the bay. The unridged ice thickness, the areal extent of ridges, and the effective (unridged plus ridged) ice thickness in the bay all increased as a function of distance from shore, i.e., from west to east.

2. Satellite passive microwave (SSM/I)-derived ice concentration data indicate that the ice conditions observed in TNB, and thus by implication the estimated heat fluxes, were normal for late May. The almost complete and ridged ice cover in the bay was probably due to the blocking effect of the high concentration, thick, and extensively ridged pack ice outside the bay. Unable to advect to the east, the ice in the bay consolidated and ridged in response to the strong westerly katabatic air flow.

3. The closure of the polynya as the ice backed up toward the coast did not shut off the heat flow from TNB. Although the bay was almost completely covered with ice, the area-weighted mean heat flux was still an order of magnitude greater than that in the adjacent pack ice. While the heat flux was locally very high in the open westernmost region of the bay, it contributed only a relatively small proportion of the area-weighted mean heat flux. The latter was dominated by the heat loss through the extensive ice cover. The heat flux in the bay was not uniformly distributed; it decreased by an order of magnitude as the ice thickness increased from west to east. Since the ice conditions observed in TNB were apparently normal for the time of year, the heat fluxes and their distribution must also have been quite normal.

This investigation suggests that much could be learned from further in situ investigations of the TNB ice cover and the adjacent pack ice. Logistical constraints to detailed in situ studies of ocean-ice-atmosphere interactions in TNB polynya clearly are not insurmountable. More detailed information on the spatial and temporal variability of ice characteristics and processes could be obtained from longer-duration ship-based studies, coupled with remote sensing, to obtain data under a wider variety of environmental and ice formation conditions than was possible during our brief excursion into TNB. By establishing more precisely the role of katabatic winds and the pack ice on ice cover variability from autumn through spring in TNB, it would be possible to make improved estimates of heat fluxes, ice and salt production, and their role in water mass modification and formation. Further field and analytical studies are vital for the improvement of numerical simulations of polynya dynamics and thermodynamics and increasing the understanding of Antarctic coastal polynyas as sites for locally high heat and salt fluxes and their impact on regional and even larger scale atmospheric and oceanic processes.

Acknowledgments. This study was supported by NSF grants OPP-9316767 and OPP-9614844. The paper was written while Jeffries was on sabbatical leave, funded in part by the Office of Naval Research, at the Department of Oceanography, U.S. Naval Postgraduate School. We thank R. Jaña, S. Li, D. Naber, J.-L. Tison, and X. Zhou for their assistance with data acquisition. Captain Joe Borkowski III and the officers and crew of the R/V *Nathaniel B. Palmer* and Antarctic Support Associates personnel contributed much to a productive cruise. The NOAA-AVHRR data used to determine cloud cover for the flux calculations were provided by the Arctic and Antarctic Research Center, Scripps Institution of Oceanography, San Diego, California. The SSM/I sea ice concentration data were provided by the NASA EOS Distributed Active Archive Center (DAAC) at the National Snow and Ice Data Center, University of Colorado, Boulder, Colorado. The automatic weather station data were provided by the Automatic Weather Station Project at the University of Wisconsin-Madison. Hajo Eicken offered helpful comments and suggestions on an early version of the paper. This final version benefited from evaluations by Stan Jacobs (Associate Editor) and his chosen reviewers: Mike Van Woert, Peter Guest, and an anonymous individual.

References

Adolphs, U., and G. Wendler, A pilot study on the interaction between katabatic winds and polynyas at the Adélie Coast, eastern Antarctica, *Antarct. Sci., 7,* 307-314, 1995.

Allison, I., and A. P. Worby, Seasonal changes of sea-ice characteristics off East Antarctica, *Ann. Glaciol., 20,* 195-201, 1994.

Andreas, E. L., A theory for the scalar roughness and the scalar transfer coefficients over snow and sea ice, *Boundary Layer Meteorol., 38,* 159-184, 1987.

Andreas, E. L., and B. Murphy, Bulk transfer coefficients for heat and momentum over leads and polynyas, *J. Phys. Oceanogr., 16,* 1875-1883, 1986.

Bromwich, D. H., and D. D. Kurtz, Katabatic wind forcing of the Terra Nova Bay polynya, *J. Geophys. Res., 89,* 3561-3572, 1984.

Bromwich, D. H., Z. Liu, A. N. Rogers, and M. L. Van Woert, Winter atmospheric forcing of the Ross Sea polynya, in *Ocean, Ice and Atmosphere: Interactions at the Antarctic Continental Margin, Antarct. Res. Ser.,* vol. 75, edited by S. S. Jacobs and R. F. Weiss, pp. 101-133, AGU, Washington, D.C., 1998.

Cavalieri, D. J., and S. Martin, A passive microwave study of polynyas along the Wilkes Land coast, in *Oceanology of the Antarctic Continental Shelf, Antarct. Res. Ser.,* vol. 43, edited by S. S. Jacobs, pp. 227-252, AGU, Washington, D.C., 1985.

Cavalieri, D. J., P. Gloersen, and W. J. Campbell, Determination of sea ice parameters with the Nimbus 7 SMMR, *J. Geophys. Res., 89,* 5355-5369, 1984.

Cox, G. F. N., and W. F. Weeks, Numerical simulations of the profile properties of undeformed first-year sea ice during the growth season, *J. Geophys. Res., 93,* 12,449-12,460, 1988.

Eicken, H., and M. A. Lange, Development and properties of sea ice in the coastal regime of the southeastern Weddell Sea, *J. Geophys. Res., 94,* 8193-8206, 1989.

Gallée, H., Air-sea interactions over Terra Nova Bay during winter: Simulation with a coupled atmosphere-polynya model, *J. Geophys. Res., 102,* 13,835-13,849, 1997.

Jacobs, S. S., and J. C. Comiso, Sea ice and oceanic processes on the Ross Sea continental shelf, *J. Geophys. Res., 94,* 18,195-18,211, 1989.

Jacobs, S. S., R. G., Fairbanks, and Y. Horibe, Origin and evolution of the water masses near the Antarctic continental margin: Evidence from $H_2{}^{18}O/H_2{}^{16}O$ ratios in seawater, in *Oceanology of the Antarctic Continental Shelf, Antarct. Res. Ser.,* vol. 43, edited by S. S. Jacobs, pp. 59-85, AGU, Washington, D.C., 1985.

Jeffries, M. O., and U. Adolphs, Early winter snow and ice thickness distribution, ice structure and development of the western Ross Sea pack ice between the ice edge and the Ross Ice Shelf, *Antarct. Sci., 9,* 188-200, 1997.

Jeffries, M. O., T. Zhang, K. Frey, and N. Kozlenko, Estimating late winter heat flow to the atmosphere from the lake-dominated Alaskan North Slope, *J. Glaciol., 45,* 315-324, 1999.

König-Langlo, G., and E. Augstein, Parameterization of the downward long-wave radiation at the Earth's surface in the polar regions, *Meteorol. Z., 3,* 343-347, 1994.

Kottmeier, C., and D. Engelbart, Generation and atmospheric heat exchange of coastal polynyas in the Weddell Sea, *Boundary Layer Meteorol., 60,* 207-234, 1992.

Kovacs, A., Sea Ice, part I, Bulk salinity versus ice floe thickness, *CRREL Rep. 96-7,* 16 pp., U.S. Army Cold Reg. Res. and Eng. Lab., Hanover, N.H., 1996.

Kurtz, D. D., and D. H. Bromwich, Satellite observed behavior of the Terra Nova Bay polynya, *J. Geophys. Res., 88,* 9717-9722, 1983.

Kurtz, D. D., and D. H. Bromwich, A recurring, atmospherically forced polynya in Terra Nova Bay, in *Oceanology of the Antarctic Continental Shelf, Antarct. Res. Ser.,* vol. 43, edited by S. S. Jacobs, pp. 177-201, AGU, Washington, D.C., 1985.

Manzella, G. M. R., R. Meloni, and P. Picco, Current, temperature and salinity observations in the Terra Nova Bay polynya area, in *Oceanography of the Ross Sea,* edited by G. Spezie and G. M. R. Manzella, pp. 165-173, Springer-Verlag, New York, 1999.

Markus, T., and B. A. Burns, A method to estimate sub-pixel scale coastal polynyas with satellite passive microwave data, *J. Geophys. Res., 100,* 4473-4487, 1995.

Markus, T., C. Kottmeier, and E. Fahrbach, Ice formation in coastal polynyas in the Weddell Sea and their impact on oceanic salinity, in *Antarctic Sea Ice: Physical Processes, Interactions and Variability, Antarct. Res. Ser.,* vol. 74, edited by M. O. Jeffries, pp. 273-292, AGU, Washington, D.C., 1998.

Massom, R. A., M. R. Drinkwater, and C. Haas, Winter snow cover on sea ice in the Weddell Sea, *J. Geophys. Res., 102,* 1101-1117, 1997.

Massom, R. A., P. T. Harris, K. J. Michael, and M. J. Potter, The distribution and formative processes of latent-heat polynyas in East Antarctica, *Ann. Glaciol., 27,* 420-426, 1998a.

Massom, R. A., V. I. Lytle, A. P. Worby, and I. Allison, Winter snow cover variability on East Antarctic sea ice, *J. Geophys. Res., 103,* 24,837-24,855, 1998b.

Morris, K., and M. O. Jeffries, Seasonal contrasts in the characteristics of the snow cover on Ross Sea ice floes, *Ann. Glaciol.,* in press, 2001.

National Snow and Ice Data Center (NSIDC), *DMSP SSM/I Brightness Temperatures and Sea Ice Concentration Grids for Polar Regions: User's Guide,* Univ. of Colo., Coop. Inst. for Res. in Environ. Sci., Boulder, 1996.

Parish, T. R., and D. H. Bromwich, Instrumented aircraft observations of the katabatic wind regime near Terra Nova Bay, *Mon. Weather Rev., 117,* 1570-1585, 1989.

Steffen, K., and A. Schweiger, NASA team algorithm for sea ice concentration retrieval from Defense Meteorological Satellite Program special sensor microwave imager: Comparison with Landsat imagery, *J. Geophys. Res., 96,* 21,971-21,987, 1991.

Sturm, M., J. Holmgren, M. König, and K. Morris, The thermal conductivity of seasonal snow, *J. Glaciol., 43,* 26-41, 1997.

Sturm, M., K. Morris, and R. Massom, Diagenesis of the winter snow cover of the west Antarctic pack ice, in *Antarctic Sea Ice: Physical Processes, Interactions and Variability, Antarct. Res. Ser.,* vol. 74, edited by M. O. Jeffries, pp. 1-18, AGU, Washington, D.C., 1998.

Sturman, A. P., and M. R. Anderson, On the sea-ice regime of the Ross Sea, Antarctica, *J. Glaciol., 32,* 54-59, 1986.

Szekielda, K. H., The hot spot in the Ross Sea: Upwelling during wintertime, *Tethys, 6,* 105-110, 1974.

Van Woert, M. L., The wintertime expansion and contraction of the Terra Nova Bay polynya, in *Oceanography of the Ross Sea: Antarctica,* edited by G. Spezie and G. M. R. Manzella, pp. 145-164, Springer-Verlag, New York, 1999a.

Van Woert, M. L., Wintertime dynamics of the Terra Nova Bay polynya, *J. Geophys. Res., 104,* 7753-7769, 1999b.

Van Woert, M. L., R. H. Whritner, D. E. Walliser, D. H. Bromwich, and J. C. Comiso, ARC: A source of multisensor satellite data for polar science, *Eos Trans. AGU, 73,* 65, 75-76, 1992.

Wamser, C., and D.G. Martinson, Drag coefficients for winter Antarctic pack ice, *J. Geophys. Res., 98,* 12,431-12,437, 1993.

Weeks, W. F., S. F. Ackley, and J. Govoni, Sea ice ridging in the Ross Sea, Antarctica, as compared with sites in the Arctic, *J. Geophys. Res., 94,* 4984-4988, 1989.

Worby, A. P., Seasonal variations in the thickness distribution and snow cover of Antarctic sea ice in the region of 60°-150°E, Ph.D. thesis, Univ. of Tasmania, Hobart, Tasmania, Australia, 1998.

Worby, A. P., and I. Allison, Ocean-atmosphere energy exchange over thin, variable concentration Antarctic pack ice, *Ann. Glaciol., 15,* 184-190, 1991.

Worby, A. P., and I. Allison, A technique for making ship-based observations of Antarctic sea ice thickness and characteristics, part I, Observational techniques and results, *Res. Rep. 14,* pp. 1-23, Antarctic CRC, Hobart, Tasmania, Australia, 1999.

Worby, A. P., M. O. Jeffries, W. F. Weeks, K. Morris, and R. Jaña, The thickness distribution of sea ice and snow cover during late winter in the Bellingshausen and Amundsen Seas, *J. Geophys. Res., 101,* 28,441-28,455, 1996.

Worby, A. P., R. A. Massom, I. Allison, V. I. Lytle, and P. Heil, East Antarctic sea ice: A review of its structure, properties and drift, in *Antarctic Sea Ice: Physical Processes, Interactions and Variability, Antarct. Res. Ser.,* vol. 74, edited by M. O. Jeffries, pp. 41-67, AGU, Washington, D.C., 1998.

World Meteorological Organization (WMO), Sea ice nomenclature, *WMO Rep. 259, Tech. Pap. 145,* 147 pp., 8 suppl., Geneva, 1970.

Wu, X., W. F. Budd, V. I. Lytle, and R. A. Massom, The effect of snow on Antarctic sea ice simulations in a coupled atmosphere-sea ice model, *Clim. Dyn., 15,* 127-143, 1999.

Zwally, H. J., J. C. Comiso, and A. L. Gordon, Antarctic offshore leads and polynyas and oceanographic effects, in *Oceanology of the Antarctic Continental Shelf, Antarct. Res. Ser.,* vol. 43, edited by S. S. Jacobs, pp. 203-226, AGU, Washington, D.C., 1985.

M.O. Jeffries, N. Kozlenko, T. Maksym, K. Morris, and T. Tin, Geophysical Institute, University of Alaska Fairbanks, 903 Koyukuk Drive, P.O. Box 757320, Fairbanks, AK 99775-7320. (martin.jeffries@gi.alaska.edu)

(Received June 21, 1999; revised May 1, 2000; accepted May 24, 2000).